

Sideband Instability and Recurrence of Kelvin Waves on Vortex Cores

David C. Samuels and Russell J. Donnelly

Department of Physics, University of Oregon, Eugene, Oregon 97403

(Received 7 December 1989)

We have been investigating the behavior of thin-core inviscid vortices of constant circulation in an effort to model quantized vortices in helium II. We have found that at $T=0$ K, Kelvin waves (standing cosine waves on vortex cores) are unstable to the buildup of sidebands. This instability is recurrent in the sense of the Fermi-Pasta-Ulam phenomenon.

PACS numbers: 67.40.Vs, 47.30.+s

Waves on quantized vortices in helium II have been studied for many years, and much has been learned, but substantial problems remain.¹ Wave excitations of single quantized vortex lines are considered to be helical disturbances which obey a dispersion relation first given by Lord Kelvin. When these waves are excited on a vortex line between fixed boundaries, a plane standing wave, called a Kelvin wave, is produced which rotates in the laboratory frame under its self-induced velocity.

The study of classical vortices, however, has revealed that classical vortex lines can sustain solitary waves; indeed Maxworthy, Hopfinger, and Redekopp have shown that in certain experiments the solitary wave may be the only wave excited.² Hasimoto has shown that for inviscid thin-core vortices, the equations of motion can be approximated by a nonlinear Schrödinger equation, and that such vortices support solitary-wave solutions.³ There is every reason to suppose that such considerations should apply to quantized vortices; indeed some unpublished experiments of our own have suggested that ions moving along quantized vortex lines might be accompanied by solitary waves. In order to design a crucial experiment we have been performing simulation studies of vortex waves. To our surprise we have discovered that Kelvin waves above a threshold amplitude are unstable at low temperatures. The origin of this claim is the subject of the present Letter.

A striking behavior of many nonlinear systems is their ability to reconstruct (or very nearly reconstruct) their initial state in a reasonably short time. This "recurrence" phenomena was first noted by Fermi, Pasta, and Ulam⁴ (FPU) in early numerical simulations of chains of nonlinear oscillations. Commonly called FPU recurrence (to distinguish this behavior from Poincaré recurrence which has practically infinite recurrence times for systems with more than a trivial number of degrees of freedom), this type of behavior is known to occur in solutions to the Korteweg-de Vries equation⁵ (KdV) and the nonlinear Schrödinger equation (NLSE).⁶ In this paper we also report our observations of recurrent behavior in simulations of thin-core, inviscid vortex dynamics.

The equation of motion of a point \mathbf{r} on a thin vortex

core is given by the Biot-Savart law,

$$\frac{d\mathbf{r}}{dt} = \frac{\Gamma}{4\pi} \int \frac{(\mathbf{r}_1 - \mathbf{r}) \times d\mathbf{r}_1}{|\mathbf{r}_1 - \mathbf{r}|^3}, \quad (1)$$

where Γ is the circulation. The common approximation to use here is the local induction method (or the Arms-Hama method),⁷

$$d\mathbf{r}/dt = G\mathbf{r}' \times \mathbf{r}'', \quad (2)$$

where we define

$$G = (\Gamma/4\pi) \ln(R_N/a_{\text{eff}}), \quad (3)$$

a prime denotes differentiation by arclength, a_{eff} is the effective core size, and R_N is an adjustable length scale. In Hasimoto's derivation of Eq. (4) and in our simulations that use the Arms-Hama approximation, the factor G is assumed constant in space and time. We employ both the full Biot-Savart law and the local Arms-Hama method in our simulations.

The NLSE derived by Hasimoto from Eq. (2) for vortex motion is

$$0 = i\Phi_t + \Phi_{ss} + \frac{1}{2} |\Phi|^2 \Phi, \quad (4)$$

where we define

$$\Phi = \kappa \exp\left(i \int_0^s \tau ds\right), \quad (5)$$

κ is the curvature of the vortex core, τ is the torsion, and s is the arclength. This formulation of the problem points the way to some interesting possible vortex behavior, though it should be kept in mind that the NLSE is only an approximation to the full Biot-Savart law. In particular, the assumption of constant G is questionable.² None of our simulations were done using the NLSE; however, the simulations using the Arms-Hama equation should be equivalent to the NLSE.

Our simulations deal with a specific vortex system: quantized vortices in liquid-helium II. This system has certain properties that make it a particularly good physical system to be modeled by Eq. (1). Superfluid helium at absolute zero is inviscid and irrotational. The circula-

tion around a vortex core is quantized ($\Gamma = h/m$, where m is the mass of the helium atom) and, due to energy considerations, only a single quantum of circulation is present in each vortex. The core radius is measured experimentally to be on the order of 1 \AA , so the core is thin. Though our simulations are done using the specific circulation and core size for superfluid helium vortices, the results reported here apply to any thin-core inviscid vortex.

In 1967, Benjamin and Feir⁸ showed that finite-amplitude waves on deep water (Stokes waves) are unstable to perturbations in the sideband waves. Later this was found to be a general instability of wave solutions to the NLSE,⁶ with applications in many fields of physics. Helical waves are wave solutions to Hasimoto's NLSE for constant curvature and constant torsion. Following the stability analysis of Andersen, Datta, and Gunshor⁹ for waves in a dispersive medium with a third-order nonlinearity, and translating to vortex-dynamics vocabulary, we find the stability condition for helical waves to be

$$A_0/\lambda < 1/2\pi n, \quad (6)$$

where A_0 is the initial amplitude of the main helical wave, λ is the wavelength, and n is the number of half waves on the vortex. Unstable sidebands will grow exponentially, with the growth exponent α ,

$$\alpha = G \left(\frac{2\pi}{\lambda n} \right)^2 \left[\left(2\pi n \frac{A_0}{\lambda} \right)^2 - 1 \right]^{1/2}, \quad (7)$$

for the nearest-neighbor sidebands. Once the sidebands grow to be comparable in magnitude to the main amplitude, this instability analysis is invalid and a new behavior (recurrence) occurs.

For our initial conditions, we started the simulations with a superposition of a planar wave and two neighboring sidebands of small amplitude as a perturbation. The vortex extended across a gap, set at 0.001 cm between two flat horizontal boundaries. The boundary conditions are that the vortex line meets the boundaries normally and can slip along the boundary. The velocity field of the vortex line must be parallel to the boundary at the boundary. These conditions were met by using the method of images. The logarithmic singularity in Eq. (1) is healed by using a finite-size hollow-core model due to Schwarz.¹⁰ The vortex line was modeled by $N=128$ straight-line vortices. We integrated both Eqs. (1) and (2) using a Runge-Kutta-Fehlberg method on an HP 835 computer, with early work done a Cray X-MP/48 computer at the San Diego Supercomputer Center.

As we integrate the equations of motion forward in time we take the wave form and do a least-squares fit of the amplitudes and phases (in the horizontal plane) of a set of 21 cosine waves ($n=0$ to 20) at fixed intervals in the number of time steps. The fits are used for data output only. In Fig. 1 we show a graph of the amplitudes versus time for a simulation using Eq. (2). The re-

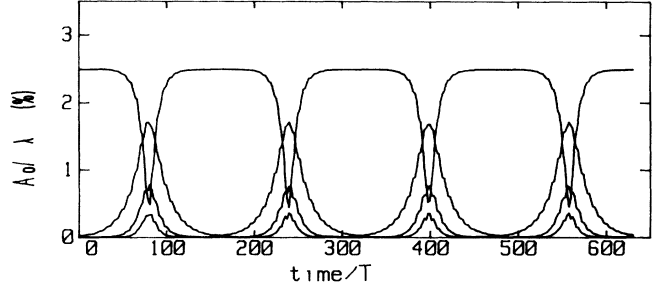


FIG. 1. Sideband instability and recurrence phenomenon for a quantized vortex line. At $t=0$ we impose a cosine wave of $n=11$ half waves at an amplitude of $A_0=0.025\lambda$ with one pair of sidebands (10 and 12 half waves) of amplitude $\tilde{A}=0.01A_0$. This Kelvin wave rotates in the laboratory frame with a period $T=2\lambda^2/\Gamma[\ln(\lambda/2\pi a_{\text{eff}})-0.116]$. Here, we plot the amplitude of the main harmonic ($n=11$) and the lower harmonics ($n=10, 9$, and 8 in order of decreasing amplitude) of the three closest sidebands as a function of time. The amplitude is scaled by the wavelength λ and the time is scaled by the period of the main initial cosine wave. A plot of the amplitude of the upper harmonics ($n=12, 13$, and 14) of the sidebands looks very similar.

currence behavior of the system is very clear and regular.

There is no known method of predicting the FPU recurrence time, though estimates can be made. A good estimate for the recurrence time in our simulation is given simply by considering the exponential growth time of the sidebands. The sideband amplitudes are observed to grow exponentially nearly all the way to a maximum and then decay exponentially back to the original perturbation amplitude (within a few percent). This gives an estimated recurrence time of

$$T_{\text{rec}} \approx \frac{2}{\alpha} \left[\ln \left(\frac{A_0}{\tilde{A}} \right) \right], \quad (8)$$

where \tilde{A} is the initial amplitude of the sidebands. The exponential behavior of the growth of the sideband amplitudes to such large values relative to the initial wave is surprising since the Benjamin-Feir approximations break down before that point. Also surprising is the fact that the recurrence involves not only recreating the original main amplitude but also recreating the perturbation amplitudes. This is a very sensitive dependence of the long-time behavior of the system to initial conditions. We can rewrite (8) as

$$T_{\text{rec}} \approx \left[\frac{(\lambda n)^2}{2G\pi} \right] \left[\frac{\ln(A_0/\tilde{A})}{\pi[(2\pi n A_0/\lambda)^2 - 1]^{1/2}} \right], \quad (9)$$

where the first term is the beat time between the main mode and the sideband modes and the term in parenthesis is of order 1 or larger for $\tilde{A} \ll A_0$. Thus the beat period can be used as an estimated lower limit for the recurrence period. Table I gives our results of simulations using the Arms-Hama approximation while vary-

TABLE I. Observed recurrence times T_{rec} , from simulations using the Arms-Hama approximation, as a function of A_0/λ and A_0/\bar{A} compared to predictions from Eq. (8). The simulation of $A_0/\lambda = 3.0$ is in the confined-chaos region but the amplitudes show enough recurrence to measure an approximate recurrence time.

A_0/λ (%)	A_0/\bar{A}	T_{rec} (simulation) (10^{-3} sec)	T_{rec} [Eq. (8)] (10^{-3} sec)
2.0	100	2.0 ± 0.1	1.5
2.5	100	1.3 ± 0.1	1.0
3.0	100	0.9 ± 0.1	0.8
2.5	20	0.8 ± 0.1	0.7

ing the ratios A_0/λ and A_0/\bar{A} , compared to the predicted values from Eq. (8). The differences are explained by the low values of α in the simulations [see Fig. 3 and Eq. (8)].

This simple FPU recurrence is not the only large-time-scale behavior of this system. If the amplitude of the main frequency is large enough then the next-nearest-neighbor sidebands also become unstable. This instability limit is given by

$$A_0/\lambda > 1/\pi n. \tag{10}$$

For amplitudes past this limit simple recurrence is not observed. Instead the energy seems to shift in a complicated manner among the unstable modes (Fig. 2). This behavior has been labeled “confined chaos” by Caponi, Saffman, and Yuen.¹¹ Our simulations verify this behavior for both the Arms-Hama approximation and the full Biot-Savart calculation.

In Fig. 3 we show the observed growth exponents of the sideband amplitudes in simulations using both the Biot-Savart law and the Arms-Hama approximation with a comparison to the theoretical prediction of Eq. (7). The difference between the theoretical exponents and the values from the simulations is apparently an artifact of the finite mesh of the simulation. We have done

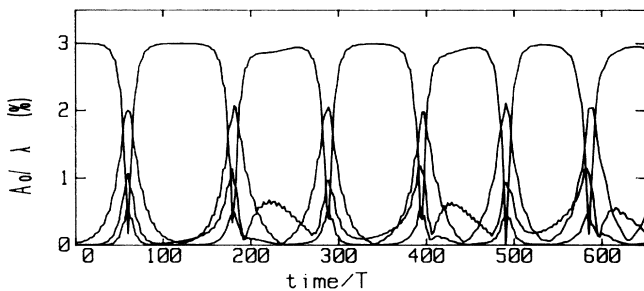


FIG. 2. The same initial conditions as Fig. 1 except that the initial amplitude of the main cosine wave is raised to $A_0 = 0.03\bar{A}$, slightly over the limit on simple recurrence [Eq. (10)]. The qualitative difference compared to Fig. 1 has been called “confined chaos.”

some simulations using a greater number of points to mesh the vortex line, and the results of these simulations approach more closely the theoretical values. Because of the very time-intensive nature of simulations using the Biot-Savart law, we have only done simulations over a range of initial amplitudes using 128 points on the line. The growth exponents from the Biot-Savart simulations fall consistently below the exponents from the Arms-Hama simulations. We do not know if this is just due to a greater effect from the meshing in the Biot-Savart calculations or if there is some actual stabilization in this case. Notice that for an amplitude of 0.015λ we do observe a small negative growth exponent for the Biot-Savart simulation.

The existence of recurrence has often been closely involved with the existence of solitons in the system, especially in the case of the KdV-equation simulations of Zabusky and Kruska⁵ where the recurrence time was determined by the relative velocities of a large number of observed solitons. In our vortex simulations we see only a single localized wave created in each recurrence cycle for wave amplitudes in the simple-recurrence range, along with a significant remnant of the periodic wave form. Here, we define a “localized wave” as a region of the vortex wave with significantly greater amplitude than the surrounding wave form. This localized wave is observed to travel along the vortex core, reflecting off the boundaries. It has not yet been rigorously identified with the Hasimoto soliton.³ When the initial wave amplitude is increased beyond the limit of Eq. (10), into the region where two pairs of sidebands are unstable, two separate localized waves are observed, again behaving like solitons. We have found no other relationship in our system

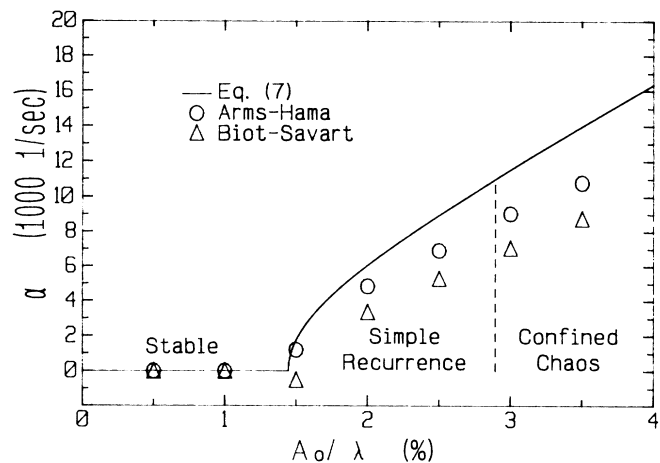


FIG. 3. Stability analysis of Ref. 7 compared to simulation. Error bars are $\leq 250 \text{ sec}^{-1}$. The values shown are the growth exponents of the $n-1$ sideband; the observed exponents for the $n+1$ sideband agree within the error for all amplitudes except the amplitude on the extreme right in the Biot-Savart simulation. There the $n+1$ exponent was 1700 sec^{-1} lower than the $n-1$ exponent.

between the recurrence behavior and the localized wave properties.

Because of the time-intensive calculations needed to solve the Biot-Savart equation, we have explored the recurrence behavior only for the Arms-Hama equation. We have run a very few long-time simulations using the Biot-Savart law to confirm that recurrence does indeed occur in this equation also.

This is the first report of the Benjamin-Feir instability and recurrent behavior on vortex cores. In addition, it provides a mechanism by which solitons can be generated on vortices, particularly in the confined-chaos region. This is also the first report of solitary-wave behavior on a quantized vortex line in ^4He , although it could have been anticipated from Refs. 2 and 3. The sideband instability and recurrence behavior are not limited to the geometry of planar waves on straight-line vortices; we have observed both phenomena in simulations of helical waves on vortex rings. The calculations reported here of Kelvin-wave instability are for a free system, not a driven system as in experiments in liquid helium. Further work is needed to learn how to describe a driven vortex wave and to couple ions, the most important microscopic probe in use today, to the vortex line. Since the dispersion relation of helical waves and solitary waves are closely related,² the observations of Ashton and Glaberson¹² of a broad resonance related to the dispersion curve of Kelvin waves do not prove that stable

Kelvin waves were generated in their experiments.

We gratefully acknowledge support from NSF Grant No. DMR-8815803, and the San Diego Supercomputing Center.

¹W. I. Glaberson and R. J. Donnelly, in *Progress in Low Temperature Physics*, edited by D. F. Brewer (North-Holland, Amsterdam, 1986), Vol. IX, Chap. 1.

²T. Maxworthy, E. J. Hopfinger, and L. G. Redekopp, *J. Fluid Mech.* **151**, 141 (1985).

³H. Hasimoto, *J. Fluid Mech.* **51**, 477 (1972).

⁴E. Fermi, J. Pasta, and S. Ulam, in *Collected Papers of Enrico Fermi*, edited by E. Segré (Univ. of Chicago, Chicago, 1965), p. 978.

⁵N. J. Zabusky and M. D. Kruskal, *Phys. Rev. Lett.* **15**, 240 (1965).

⁶H. C. Yuen and W. E. Ferguson, Jr., *Phys. Fluids* **21**, 1275 (1978).

⁷R. J. Arms and F. R. Hama, *Phys. Fluids* **8**, 553 (1965).

⁸T. B. Benjamin and J. E. Feir, *J. Fluid Mech.* **27**, 417 (1967).

⁹D. R. Andersen, S. Datta, and R. L. Gunshor, *J. Appl. Phys.* **54**, 5608 (1983).

¹⁰K. W. Schwarz, *Phys. Rev. B* **31**, 5782 (1984).

¹¹E. A. Caponi, P. G. Saffman, and H. C. Yuen, *Phys. Fluids* **25**, 2159 (1982).

¹²R. A. Ashton and W. I. Glaberson, *Phys. Rev. Lett.* **42**, 1062 (1979).